Laser-induced ferroelectric domain engineering in $LiNbO_3$ crystals using an amorphous silicon overlayer

G. Zisis[1], G. Martinez-Jimenez[1], Y. Franz[1], N. Healy[2], T. M. Masaud[3], H. M. H. Chong[3], E. Soergel[4], A. C. Peacock[1], S. Mailis[1]

[1]Optoelectronics Research Centre, University of Southampton, Southampton, SO17 1BJ, U.K.
[2]School of Electrical and Electronic Engineering, Merz Court, Newcastle University, Newcastle upon Tyne, NE1 7RU, UK
[3]School of Electronic and Computer Science, University of Southampton, Highfield, Southampton SO17 1BJ, U.K.
[4]Institute of Physics, University of Bonn, Wegelerstrasse 8, 53115 Bonn, Germany

E-mail: sm@orc.soton.ac.uk

Abstract. We report laser-induced poling inhibition and direct poling in lithium niobate crystals ($LiNbO_3$), covered with an amorphous silicon (a-Si) light-absorbing layer, using a visible (488 nm) continuous wave (c.w.) laser source. Our results show that the use of the a-Si overlayer produces deeper poling inhibited domains with minimum surface damage, as compared to previously reported UV laser writing experiments on uncoated crystals, thus increasing the applicability of this method in the production of ferroelectric domain engineered structures for nonlinear optical applications. The characteristics of the poling inhibited domains were investigated using differential etching and piezoresponse force microscopy.

PACS numbers: 42.70.Mp, 77.84.Ek, 42.10

Keywords: ferroelectric domain inversion, nonlinear crystals, lithium niobate, laser processing

1. Introduction

Ferroelectric domain engineered $LiNbO_3$ crystals are commonly used for efficient wavelength conversion by quasi-phase-matching, [1, 2, 3] all-optical signal processing [4], surface and bulk micro-structuring [5, 6], optical performance improvement of photonic devices [7] and generation of surface acoustic waves (SAW) [8]. Ferroelectric domain inversion in $LiNbO_3$ crystals is achieved conventionally by the application of an external

electric field exceeding the coercive field. Spatially selective domain inversion can be achieved by electrode shaping, which creates a spatial modulation of the electric field amplitude. In addition to the conventional methods to achieve spatially selective domain inversion, there are reports of laser assisted methods where a spatial modulation of the coercive field can be achieved. In the case of un-doped congruent $LiNbO_3$, such light-mediated domain engineering techniques as light-assisted poling [9], all-optical poling [10], and poling inhibition [11], have been successfully reported for producing solid, arbitrary shaped, sub-micron domains.

Poling inhibition (PI) employs UV laser irradiation of the +z face of the crystal, where an increase of the coercive field is observed locally as a result of the migration of lithium ions. In a subsequent step of uniform electric field poling of the crystal, a small volume of the crystal directly below the irradiated surface maintains its domain orientation resulting in a spatially selective domain pattern, which is associated to the UV irradiated track. The first demonstration of PI [11] involved irradiation with a 244 nm laser, which corresponds to radiation strongly absorbed by the crystal itself producing steep temperature gradients resulting in lithium diffusion. UV laser irradiation of the -z polar face of the crystal generates a bipolar electric field [12] that is sufficiently high to induce *direct poling*.

Variations of direct poling have been reported in the literature where UV (244 nm) [13], and visible laser sources (488 nm) [14] were used to irradiate a Chromium (Cr) covered polar face of a $LiNbO_3$ sample. The thin layer ($\sim$40 nm) of Cr was used to facilitate the absorption of laser radiation. It was found that the Cr overlayer protected the surface of the crystal from laser-induced surface damage but also resulted in chemical reduction of $LiNbO_3$ and oxidation of the Cr layer. Chemically reduced $LiNbO_3$ has the same piezoelectric properties as the congruent crystal, therefore it can still be used for generation and propagation of surface acoustic waves. It exhibits however a dramatic increase in optical absorption thus compromising the utility of the crystal for photonic applications.

Here, we present experimental results in which an a-Si light-absorbing layer is introduced to obtain (surface damage free) poling inhibition and to reproduce direct poling results (previously obtained with UV laser irradiation of uncovered surfaces) without the restricting effects of the chemical reduction of the crystal. The absorption length in a-Si at λ=488 nm is 30 nm [15], ensuring that a thin film of $\sim$400 nm will absorb efficiently the incident visible laser radiation producing enough heat to locally raise the temperature to levels as high as the melting point of a-Si. This was shown in [15] where melting of the core of a Si-filled silica micro-capillary by visible laser irradiation lead to crystallisation of the semiconductor core.

2. Experimental arrangements

2.1. a-Si film deposition

In our experiments we used z-cut, undoped congruently melt $LiNbO_3$ crystals (Crystal Technology, Inc., US) with a thickness of 500 μm. Thin films of a-Si were deposited on the polar faces of the crystal using the method of plasma enhanced chemical vapour deposition (PE-CVD)[16]. We performed our experiments on films with thickness varying from ∼250 to ∼400 nm, with similar results. We, however, used 400 nm thick films for our systematic study, on the assumption that a thicker film will protect more efficiently the structural integrity of $LiNbO_3$ crystal surface. The deposition was performed at ∼350 °C to ensure that the deposited material is amorphous. Moreover, this temperature is sufficiently low to ensure that the $LiNbO_3$ substrate is not affected by the heat in any way. Slow cooling of the substrate after deposition however, is important to ensure that no spontaneous domain inversion, due to the pyroelectric effect, takes place. Nanodomains that are formed by fast cooling disrupt the smooth domain wall movement that is required in the poling inhibition process.

2.2. Laser irradiation

Direct laser writing of the samples was performed using a c.w. Coherent Innova Sabre 25/7 argon ion laser at λ=488 nm. The samples were scanned along linear tracks in front of the focussed laser beam using a computer-controlled high precision translation stage. The scanning speed determines the dwell time of the laser beam and the cooling rate of the laser-heated volume. In our experiments the scanning speeds used were in the range between 0.01 and 1 mm/s. The tracks were directed along the y- crystallographic axis of the crystal. The range of laser intensities used in these experiments was 0.2-1.6 MW/cm^2 using a beam diameter of ∼5 μm. The higher intensity marks the laser-induced damage threshold of the a-Si film while the lower limit marks the lowest power that produces a visible change to the a-Si surface when inspected with an optical microscope.

2.3. Poling inhibition and direct poling

To achieve poling inhibition the samples that were previously irradiated on the +z face are uniformly domain inverted by the application of a uniform electric field between the two polar surfaces. At this stage the bulk of the crystal domain inverts apart from a small volume below the laser-irradiated tracks where poling inhibition is observed. A specially designed poling cell enabled the application of an electrostatic voltage across the two polar faces, using liquid electrodes that conform to the surface of the crystal. The voltage was ramped at a rate of 2 kV/min to 10.1 kV, corresponding to an electric field of 20.2 kV/mm across the 0.5 mm thick sample. This slow rate used for increasing the amplitude of the applied electric field ensures that domain inversion occurs slowly, which is desirable since the kinetics of the domain wall motion is seen to influence greatly the shape and quality of the resultant structures. Details of the experimental

setup that was used for the uniform poling can be found in [11]. For direct poling there is no requirement for application of an external electric field as the laser irradiation itself is sufficient to cause local domain inversion on the -z face [10].

3. Results

3.1. Poling inhibition after a-Si film removal

In this case the electric field poling step that is required for PI was performed after removal of the a-Si film (using KOH). The depths and widths of the PI domains that were formed under the laser irradiated tracks were investigated using scanning electron microscopy (SEM). A wedge-polishing method combined with brief etching in HF acid was employed to enable the detailed investigation of the undersurface domain structure by stretching the depth profile along the direction of the domain [17]. A set of SEM images ofthe PI domains that were obtained at different laser irradiation conditions are shown in Fig.1. The illustrated domains were fabricated using a writing speed of 0.1 mm/s and laser beam intensities within the range of 0.28 to 0.84 MW/cm^2. The white dash line indicates the change of slope due to wedge polishing. The actual domain depth is equal to the length of the triangular domain portion below the white dash line, as measured on the SEM image, divided by 10. Some limited surface damage can be observed in the tracks that correspond to laser intensities above 0.56 MW/cm^2 at this writing speed.

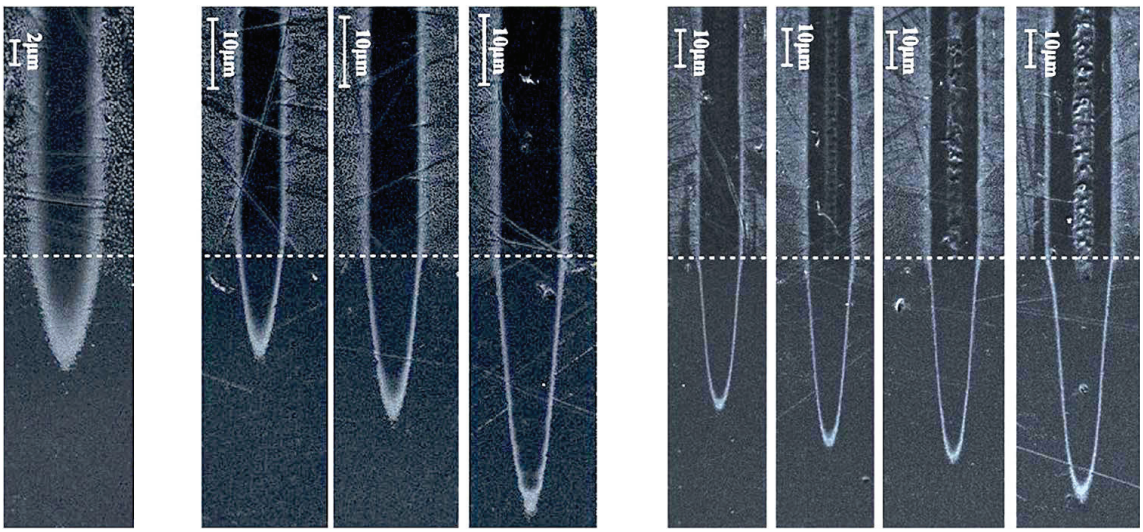

Figure 1. SEM images of wedge-polished PI sample showing domains fabricated using different laser intensities at a scanning speed of 0.1 mm/s. The corresponding laser intensities are, from left to right: 0.28, 0.35 0.42, 0.49, 0.56, 0.70, 0.77 and 0.84 MW/cm^2. The white dash line marks the change of slope due to wedge polishing. Note that the magnification is different in the three image groups.

Piezoresponse force microscopy (PFM) maps the piezoelectric response of the surfaces, which depends on the ferroelectric domain orientation. In $LiNbO_3$ there are

just two possible ferroelectric domain orientations that are expected to be represented by uniformly shaded areas with specific grey level contrast between them. PFM investigation was performed on the wedge polished section of a PI processed sample. The PFM images that are shown in Fig.2(a) and (b) confirm the formation of PI domains below the laser irradiated track. The two images correspond to PI domains that were produced using laser irradiation intensity below 0.56 MW/cm^2 (Fig.2a) and above 0.56 MW/cm^2 (Fig.2b). The PFM image in Fig.2(a) shows a region, corresponding to the PI domain, with a solid uniform shade with respect to the surrounding area. The domain shown in Fig.2(b) however, contains an area of a lighter shade, with a grey level between these corresponding to ferroelectric domains. This lighter shaded area, which follows the general shape as the domain itself but only extends to a depth of $\sim$2 μm, corresponds to reduced piezoelectric response associated with the portion of the crystal that sustained laser damage.

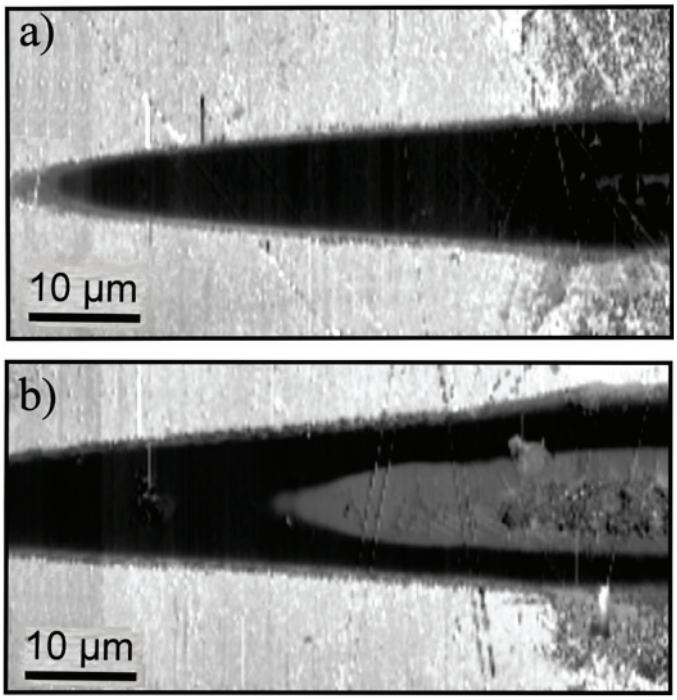

Figure 2. PFM images corresponding to PI domains fabricated with laser intensity a) below 0.56 MW/cm^2 and b) above 0.56 MW/cm^2.

The depths and widths of the PI domains that were measured on the SEM images of the wedge-polished sections are shown in the plots of Fig.3 as a function of laser irradiation intensity for three different scanning speeds. The plots indicate a linear dependence of domain depth and width with intensity. Unsurprisingly, longer dwell times of the laser beam, which corresponds to slower speeds result in deeper/wider domains, as longer heating duration results in further movement of Li ions. Special symbols used in the plots indicate the presence of surface damage. The deepest solid PI domain without any surface damage that was obtained has a depth of 3.8

$\sim$ corresponding to a laser intensity of $\sim$0.56 MW/cm^2.

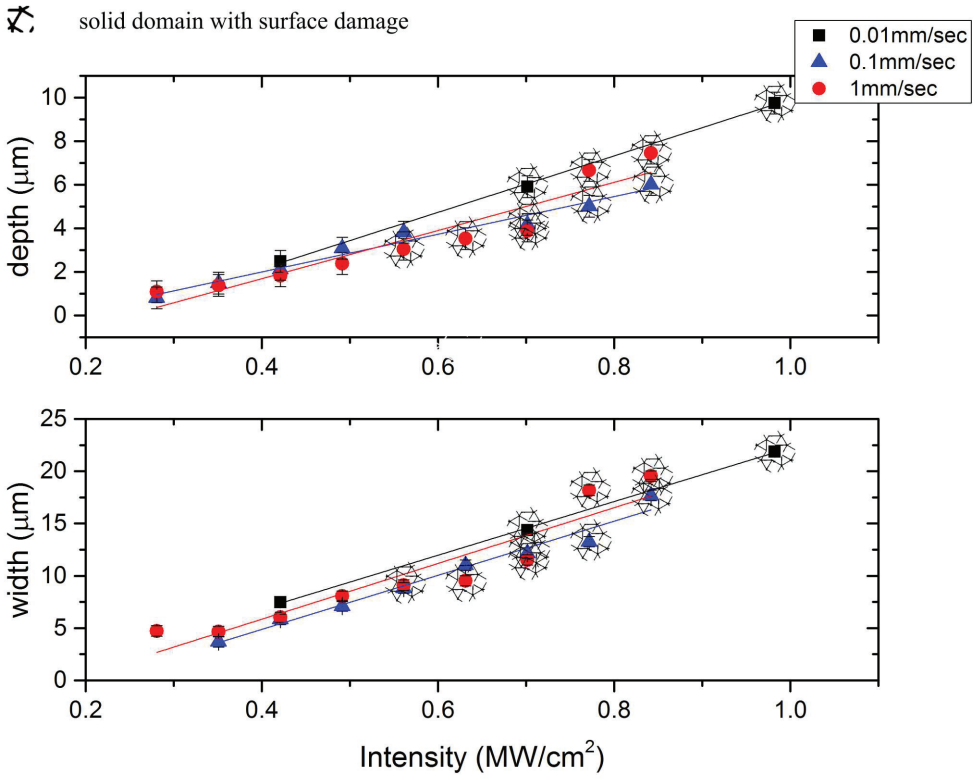

Figure 3. Depth (a) and width (b) of PI domains as a function of the writing laser intensity for different scanning speeds (0.01, 0.1 and 1 mm/s). The special symbol (shown on top left of the figure), which is superimposed to the data points indicate laser-induced surface damage.

The widest PI domain, corresponding to a solid domain without surface damage, was measured to be $\sim$10 μm. This is almost double the size of the spot size used, suggesting that the heat diffuses well beyond the irradiated area due to a fast lateral diffusion of heat in the a-Si film. The latter statement stems from a comparison to previous UV laser irradiation experiments where the resulting domain widths were close to the width of the irradiating laser beam.

The impact of the scanning speed on the domain size is shown more clearly in Fig.4, which shows a plot of the domain depths (a) and widths (b) as a function of scanning speed for two different laser intensities (I_1=0.7 MW/cm^2 and I_2=0.42 MW/cm^2). The scanning speeds were 0.01, 0.1 and 1 mm/s. The main observation here is that the intensity is the most important domain size defining parameter for speeds faster than 0.1 mm/s. Much slower speeds (0.01 mm/s) have a higher impact on the domain size.

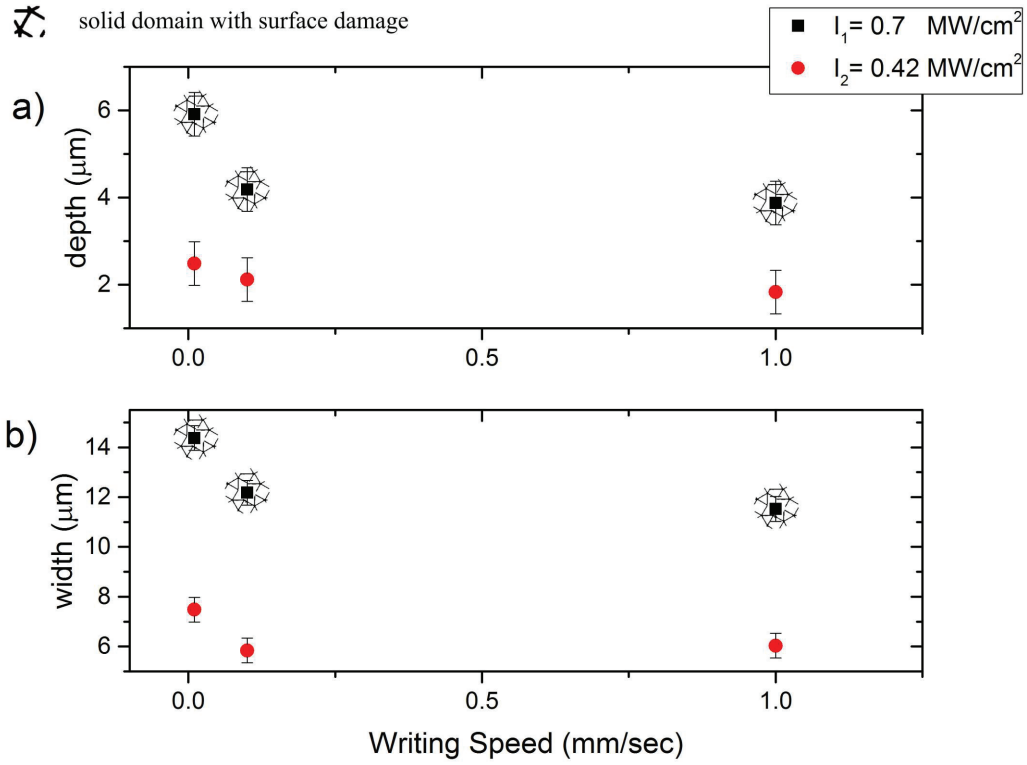

Figure 4. Depth (a) and width (b) of PI domains as a function of the laser writing speed for two laser intensities (I_1=0.7 MW/cm^2 and I_2=0.42 MW/cm^2). The special symbol (shown on top left of the figure), which is superimposed to the data points mark laser-induced surface damage.

3.2. Poling inhibition without removing the a-Si film

Assuming that the thin a-Si film is sufficiently conductive and uniform to allow the application of an external electric field we explored the possibility of performing the poling step of the PI process with the film in place. An a-Si/$LiNbO_3$ sample was prepared and irradiated locally, using a laser beam diameter of 7 μm (as in the previous experiments) and laser intensity in the range of 0.35-1.06 MW/cm^2. The range of scanning speeds used was 0.01-0.2 mm/s. The subsequent poling process was visualised in-situ using the stress-induced birefringence at the domain walls.

Random domain nucleation was observed initially along the irradiated regions followed by a subsequent domain expansion and merging as in the case of the PI process in unclad crystals. The general observation was that the size/width of these PI domains was very similar to the ones obtained in the unclad crystal case. An SEM image of the wedge-polished and etched section of the PI sample is presented in Fig.6 showing different aspects of a deep, solid PI domain. The PI domain corresponds to a laser intensity of 0.51 MW/cm^2 and writing speed of 0.016 mm/s and looks identical in shape to PI domains that were formed in unclad crystals, indicating that the PI fabrication process is not affected by the presence of the a-Si film.

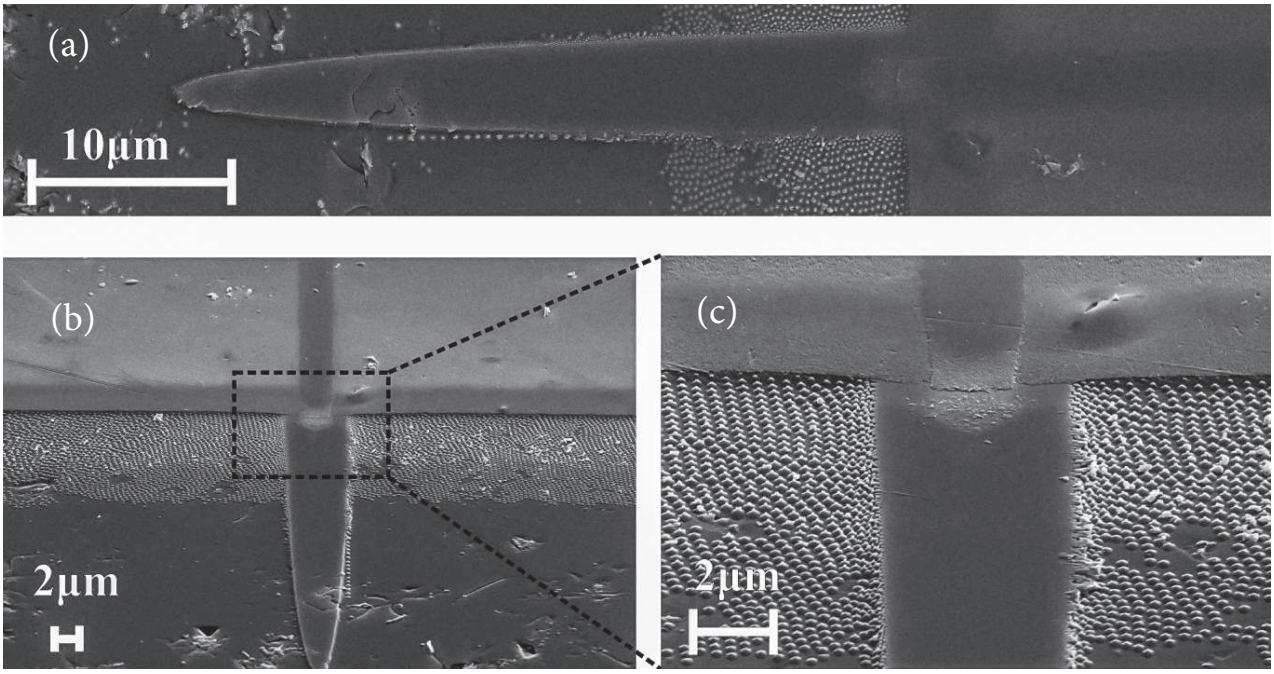

Figure 5. SEM images of the wedge-polished PI domains fabricated in (+z) a-Si/$LiNbO_3$ sample under laser intensity of 0.51 MW/cm^2 and writing speed of 0.016 mm/s. a) top view, b) tilted view at 60° and c) detail of the Si/$LiNbO_3$ interface.

Moreover, the wedge polished section reveals an assembly of sub-μm size etch-resistant features, which are visible up to a depth of ∼0.7 μm. They appear to be evenly distributed below the surface of the uniformly poled (through the a-Si film) crystal. These features are associated with poling through the a-Si film but their origin has not been identified yet. The SEM image of Fig.5 shows a distinct linear track with a different contrast on the Si film that corresponds to the laser-irradiated track. The difference in contrast is associated with laser-induced crystallisation of the a-Si film, which was verified by Raman spectroscopy of the laser irradiated part of the Si film. The shrinkage of the laser-irradiated area that can be observed in Fig.5 (b) and (c) also points to laser induced crystallisation as crystalline Si occupies a smaller volume as compared to a-Si. Finally Fig.5 reveals that the width of the laser-crystallised Si track is narrower compared to the corresponding width of the PI domain that appears below the track.

3.3. Direct poling

Here, we investigated the formation of direct domain formation as a result of laser irradiation of the a-Si clad -z crystal face. The $LiNbO_3$ samples were irradiated using a range of conditions (power and scanning speed) and the domain formation was evaluated by SEM imaging of the wedge-polished/etched surface. Fig.6(a), (b) and (c) shows the sub-surface profiles of inverted domains that were obtained with I_1=0.56 MW/cm^2, I_2=0.70 MW/cm^2 and I_3=0.84 MW/cm^2, respectively, using a scan speed of 0.01 mm/s.

The depth of the directly poled domains below the surface damage threshold is less than 1 μm. Substantial laser induced damage of the crystal is observed at higher laser intensities.

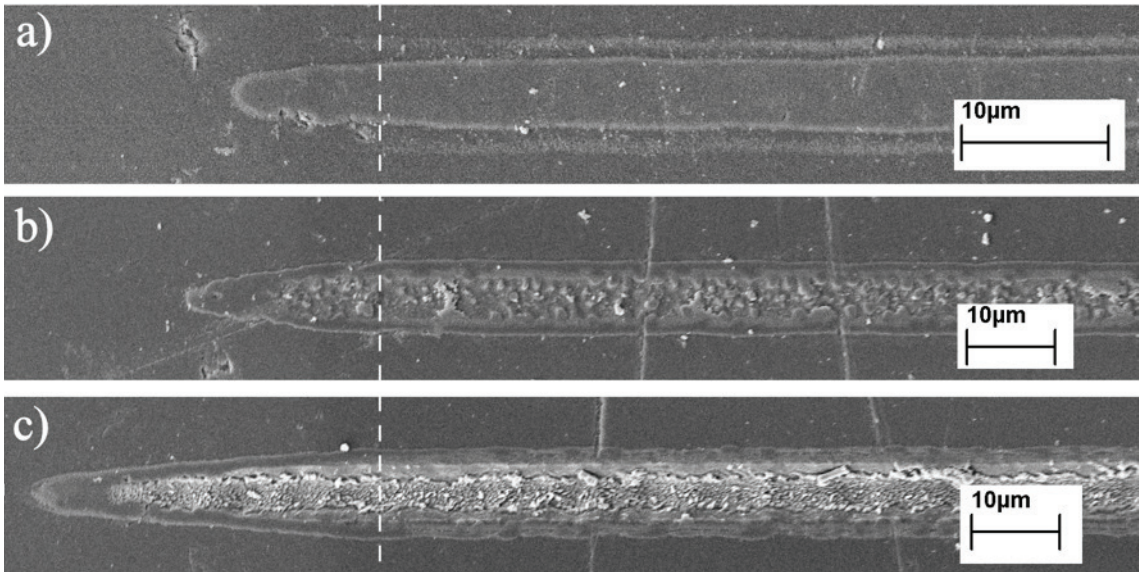

Figure 6. SEM images of the wedge-polished/etched surface showing domains formed under the laser-irradiated -z faceof an a-Si/$LiNbO_3$ sample using (a) I_1=0.56 MW/cm^2, (b) I_2=0.70 MW/cm^2 and (c) I_3=0.84 MW/cm^2, at a scan speed of 0.01 mm/s.

4. Discussion

The experimental results can be largely interpreted similarly to the case of UV laser-induced poling inhibition where direct absorption of the laser radiation by the crystal results in localised heating. The localised manner of the heating forms a steep temperature gradient ranging from melting temperature (at the centre of the laser spot size) to room temperature at a few microns away from the centre of the laser spot [18]. These steep temperature gradients cause thermal diffusion of lithium ions in the crystal that lead to poling inhibition on the +z face, which is caused by the electrostatic interaction between the propagating domain wall and the modified local electrostatic environment that has been modified due to the lithium ion redistribution under the influence of the temperature gradients [19]. The interpretation of the direct domain inversion was based on the setup of a bipolar field that also originates from the local heating [20].

In our experiments, the energy associated with the laser radiation is coupled to the a-Si overlayer rather than the $LiNbO_3$ crystal itself ($LiNbO_3$ is transparent at λ=488 nm [21]), which then transfers, in the form of heat, to the crystal underneath. In this respect, it is expected that the lateral temperature distribution in $LiNbO_3$ will be affected by the presence of the a-Si overlayer as compared to the direct UV absorption case. Additionally, the use of an overlayer makes the surface less prone to laser damage, as was shown in [13, 14]. The poling step was performed i) after and ii) prior to the removal of the a-Si film. The process of laser-induced poling inhibition is schematically

illustrated in Fig.7. A temperature gradient is being formed in the crystal as a result of localised heating of the a-Si laser-absorbing layer (a), which results in a redistribution of lithium ions (b) that modifies the coercive field locally. As lithium ions diffuses away from the peak of the temperature distribution the coercive field will increase in this part of the crystal. Finally, application of an external electric field reverses the ferroelectric domains in the bulk of the crystal minus the volume where the coercive field has been modified due to the lithium redistribution (c). The arrows indicate the direction of the spontaneous polarisation.

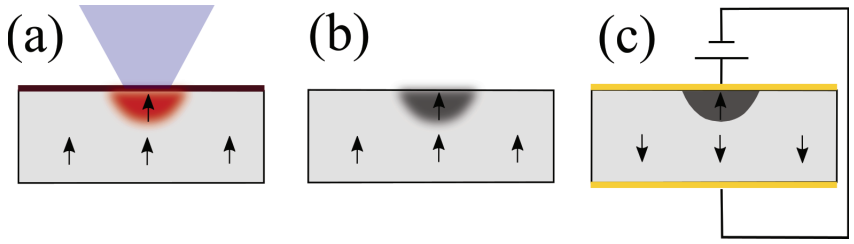

Figure 7. Schematic illustrating the poling inhibition process; a) laser irradiation of the a-Si covered +z face of the crystal, b) lithium redistribution, c) poling inhibition by applying a uniform electric field. The arrows indicate the direction of the spontaneous polarisation.

Our results show that the values for the depth and width of the PI domains that are obtained in a-Si clad $LiNbO_3$ crystals (Fig.2) are systematically larger than the ones observed in uncoated crystals with UV laser irradiation [17] with much reduced surface damage. In fact, the a-Si cladding allowed for the use of significantly higher laser powers without major surface damage. Higher laser power corresponds to a higher temperature and therefore to a longer range of lithium ions transit thus justifying the formation of deeper domains. In previous work associated with direct absorption of UV radiation, it was assumed that the surface temperature of the crystal reached the melting temperature for $LiNbO_3$. This assumption was made because of the extent of laser-induced damage that was observed. However, it is possible that the surface damage that was observed in unclad crystal experiments is associated with mechanical effects related to fast cooling. The suppression of laser-induced surface damage on the a-Si clad crystals that was observed here can be attributed to a combination of: i) mechanical strengthening of the surface, ii) flattening of the heat distribution in the film and finally, iii) modification (reduction) of the cooling rate of the crystal due to the a-Si overlayer.

The temperatures that the irradiated materials reach can be estimated by observing the SEM images shown in Fig.5. The region of the film that correspond to the laser irradiated track has a different contrast in the SEM image and also appears to be thinner with respect to the rest of the film. The change in volume is an indication of increase in density that can be associated with formation of Si crystals in that region. Independent investigation using Raman spectroscopy verified that the film in that area is indeed polycrystalline. Crystallisation of the film implies localised melting of the a-Si film, which occurs at a temperature of T_m=1,420 °K [22]. Interestingly, the extent of the

PI domain is visibly wider in comparison to the crystallised Si track, which indicates that the range of temperatures required for the formation of PI domains is significantly smaller than T_m.

Qualitatively and quantitatively, the PI domains that are formed when poling is performed before the removal of the a-Si film are similar to the ones formed when poling is performed after removal of the film. Although the scanning speed that was used in these two experiment was different, it did not impact significantly the PI domain dimensions as expected.

The experimental observations relating to *direct poling* (irradiation of the -z face) show that the domain depth achieved by irradiation of the a-Si film clad surface was limited and required higher laser intensities as compared to the results reported in [13, 14] where a Cr thin film coating was used for the same purpose. The depth of directly poled domains formed without any surface damage, shown in Fig.6a, was measured to be less than 1 μm and required much higher laser intensities, as compared to corresponding directly poled domains reported in [13]. Further increase of the laser intensity lead to the formation of deeper structures, however the surface damage was severe as shown in Fig.2(b) and (c). Interestingly, the undamaged domain size does not seem to increase significantly with increasing laser intensity (Fig.2 (a), (b) and (c)).

Finally, unlike the Cr film experiments reported in [13] here there is no oxidation of the a-Si film after laser irradiation and no chemical reduction of the crystal underneath. Raman spectroscopy revealed that the a-Si overlayer was not oxidised but became crystallised as a result of the laser irradiation. Additionally, no darkening of the crystal surface, underneath the irradiated areas, was observed after the removal of the overlayer. The lack of chemical reduction combined with the observed direct poling performance when an a-Si film is used confirms the importance of chemical reduction in the direct laser domain inversion method.

5. Conclusions

Laser-induced poling inhibition in $LiNbO_3$ crystals coated with a thin film of a-Si has been shown to produce deep domains (up to 8 μm) as well as reducing the unwanted laser-induced surface damage that was reported in previous work on UV laser-induced PI in unclad crystals. The use of such a laser absorbing overlayer enhances significantly the utility of the PI method for the fabrication of domain structures for nonlinear optical applications in lithium niobate crystals. The absorption of laser light within the overlayer confirms the hypothesis that PI is based on a thermal diffusion process powered by the steep temperature gradients that are formed by the localised laser heating. Unlike the case of Cr overlayers, there was no observation of chemical reduction of the crystal as a result of laser irradiation, which maintained the useful optical properties of the crystal but limited the efficiency of the direct poling process on the -z face. Finally, visible laser irradiation of the a-Si film led to a transition of the phase of the film from amorphous to polycrystalline, which opens up interesting opportunities for creating

$Si/LiNbO_3$ heterostructures.

6. References

[1] Miller G D, Batchko R G, Tulloch W M, Weise D R, Fejer M M and Byer R L 1997 *Opt. Lett.* **22** 1834

[2] Lim E J, Fejer M M, Byer R L and Kozlovsky W J 1989 *Electron. Lett.* **25** 731

[3] Busacca A C, Sones C L, Eason R W and Mailis S 2004 *Appl. Phys. Lett.* **84** 4430

[4] Langrock C, Kumar S, McGeehan J E, Willner A E and Fejer M M 2006 *J. Lightwave Technol.* **24** 2579

[5] Sones C, Mailis S, Apostolopoulos V, Barry I E, Gawith C, Smith P G R and Eason R W 2002 *J. Micromech. Microeng.* **12** 53–57

[6] Zisis G, Ying C Y J, Soergel E and Mailis S 2014 *J. Appl. Phys.* **115**

[7] Boyland A J, Mailis S, Hendricks J M, Smith P G R and Eason R W 2001 *Opt. Commun.* **197** 193

[8] Yudistira D, Benchabane S, Janner D and Pruneri V 2009 *Appl. Phys. Lett.* **95** 052901

[9] Sones C L, Valdivia C E, Scott J G, Mailis S, Eason R W, Scrymgeour D A, Gopalan V, Jungk T and Soergel E 2005 *Appl. Phys. B* **344** 341–344

[10] Muir A C, Sones C L, Mailis S, Eason R W, Jungk T, Hoffman A and Soergel E 2008 *Opt. Ex.* **16** 2336

[11] Sones C L, Muir A C, Ying Y J, Mailis S, Eason R W, Jungk T, Hoffmann Á and Soergel E 2008 *Appl. Phys. Lett.* **92** 72905

[12] Steigerwald H, Lilienblum M, von Cube F, Ying Y J, Eason R W, Mailis S, Sturman B, Soergel E and Buse K 2010 *Phys. Rev. B* **82**

[13] Boes A, Yudistira D, Crasto T, Steigerwald H, Sivan V, Limboeck T, Friend J, Mailis S, Soergel E and Mitchell A 2014 *Opt. Mat. Ex.* **4** 241

[14] Boes A, Sivan V, Ren G, Yudistira D, Mailis S, Soergel E and Mitchell A 2015 *Appl. Phys. Lett.* **107** 1–5

[15] Healy N, Mailis S, Bulgakova N M, Sazio P J, Day T D, Sparks J R, Cheng H Y, Badding J V and Peacock A C 2014 *Nature Materials* 1122–1127

[16] Jansen F and Krommenhoek S 1994 *Thin Solid Films* **252** 32

[17] Ying C Y J, Daniell G J, Steigerwald H, Soergel E and Mailis S 2013 *J. Appl. Phys.* **114**

[18] Muir A, Daniell G, Please C, Wellington I, Mailis S and Eason R 2006 *Appl. Phys. A* **83** 389–396

[19] Ying C Y J, Muir A C, Valdivia C E, Steigerwald H, Sones C L, Eason R W, Soergel E and Mailis S 2012 *Laser & Photon. Rev.* **6** 526

[20] Steigerwald H, Ying Y J, Eason R W, Buse K, Mailis S and Soergel E 2011 *Appl. Phys. Lett.* **98** 62902

[21] Prokhorov A and Kuz'minov Y 1990 *Physics and Chemistry of Crystalline Lithium Niobate* (Bristol and New York City: Adam Hilger)

[22] Bovatsek J, Tamhankar A, Patel R, Bulgakova N M and Bonse J 2010 *Thin Solid Films* **518** 2897–2904